Manifestation of land surface albedo and temperature dynamics towards land cover.

SALLEH, S.A., LATIF, Z.A., MOHD, W.M.N., CHAN, A., ARIFFIN, I.M. and MUSTAHA, E.

2022

MANIFESTATION OF LAND SURFACE ALBEDO AND TEMPERATURE DYNAMICS TOWARDS LAND COVER

Siti Aekbal Salleh*[1,2], Zulkiflee Abd Latif[1,2], Wan Mohd Naim Wan Mohd[2], Andy Chan[3], Imran Mohamad Ariffin[4] and Emad Mustaha[5]

[1]*Institute for Biodiversity and Sustainable Development, Universiti Teknologi MARA, 40450, Shah Alam, Selangor, Malaysia.*

[2]*Center of Studies Surveying Science and Geomatics, Faculty of Architecture, Planning and Surveying, Universiti Teknologi MARA, 40450 Shah Alam, Selangor, Malaysia.*

[3]*Faculty of Engineering, University of Nottingham Malaysia Campus, Jalan Broga, Semenyih, Selangor, Malaysia.*

[4]*ESRI Malaysia Sdn. Bhd, Unit 3A-1, Level 3A, Tower 2B, UOA Business Park No, 1, Jalan Pengaturcara U1/51a, Seksyen U1, 40150 Shah Alam, Selangor, Malaysia.*

[5]*Architectural Engineering, College of Engineering, University of Sharjah, UAE.*

Abstract

Land surface albedo studies have always been dominated by the snow-covered area while snow-free area albedo effects induced by the land use and land covers are much less documented. The objective of this study is to investigate the significant differences of land surface albedo (LSA) and land surface temperature (LST) across the multiple types of land use and land cover (LULC) using remote sensing technique. Single way ANOVA Post Hoc Tukey's Honesty Significance Difference (HSD) test was conducted to perform 25 comparisons of five (5) land use land covers. The LSA, LST and LULC data were acquired and prepared through remote sensing techniques, thus each gridded values of LULC classifications can be used to extract the pixel values of LSA and LST consistently. There are significant differences in term of values of LSA and LST across the LULC In the year 1999, the LSA of groups 3 and 5 were not statistically significant (mean difference of ±0.0000756) and the LST of groups 4 and 5 differences were also not statistically significant (mean difference of ±0.0281855). For the year 2009, the LST of groups 2 and 5, and 3 and 4 were not statistically significant with mean differences of ±0.0293095 and ±0.1000526 respectively. As for 2006, the LSA and LST of all groups of land cover appeared to be statistically significant ($p < 0.00048$) while in 2011 only one LST comparison (groups 4 and 5) appeared to be not significantly difference with a mean difference of ±0.0813049, which indicates that the land use from these groups does not significantly influence the fluctuation of LST in this region. Thus, the result in this study indicates that, it is important to quantify LSA and even the snow free region have a significant difference value of albedo. Hence, as it has been recorded as an Essential Climate Variables, it is crucial for climate researcher especially in the snow free region to also include and calibrates this bio-geophysical response of land surface variable in their simulation and research studies.

Keywords: *remote sensing; albedo; land use land cover; urban climate.*

INTRODUCTION

The reflectivity of a surface is highly dependent on the surface covers, types, colours and materials. The landscape heterogeneity can influence a variety of land surface processes and its ecological responses. Climate condition of each cities differs according to their locational setting and their land surface process. In modelling the climate condition of urban area specifically, there are many physical aspects of the local features need to be considered. Land use land cover (LULC) has high sensitivity effect towards formation of land surface albedo (LSA). The variations of LULC interact differently with solar radiation in terms of the chemical and physical properties. Thus, the basic indicator of reflectivity strength over the Earth's surface can be identified by recognising the LULC. The importance of LSA quantification comes with the essential needs for a reasonably good archive of spatial and

temporal LSA data as an essential climate variable (ECV), particularly for the benefit of surface radiation, energy balance and climate change study (Feng et al., 2022). Buyantuyev and Wu (2010) used stratifying temperature grids across the LULC technique to examine the magnitude and temporal variability of urban heat island (UHI) phenomenon and Salleh et al. (2013) have explained the influence of LULC to the formation of UHI in Putrajaya. The relationship was established by using the ordinary least square (OLS) and geographical weighted regression (GWR).

Land surface albedo can be quantified using two modes i.e., in-situ observations using handheld or permanently installed albedo-meter or by using quantitative land surface remote sensing techniques through relative model derived from satellite reflectance. The remote sensing techniques and technology of land surface albedo derivation was reviewed in Salleh et al. (2012). LULC of the selected study area (relatively cloud- free region of Putrajaya) was briefly discussed in Salleh et al. (2013). Figure 1 shows the LULC map generated from this study. The fluctuation of these land use classes can be seen in Figures 1 and 2: Even though urbanisation expanded each year; by 16% in 2006 and 5% in 2009, forested areas seemed to be the main victim as 22% of the initially forested areas decreased to just 5%. 2006 showed signs of devastation, with a 12% and 3% reduction in forested and green areas, Putrajaya managed to recuperate the situation in 2009. The green areas managed to counterbalance the adverse effects of urban deforestation.

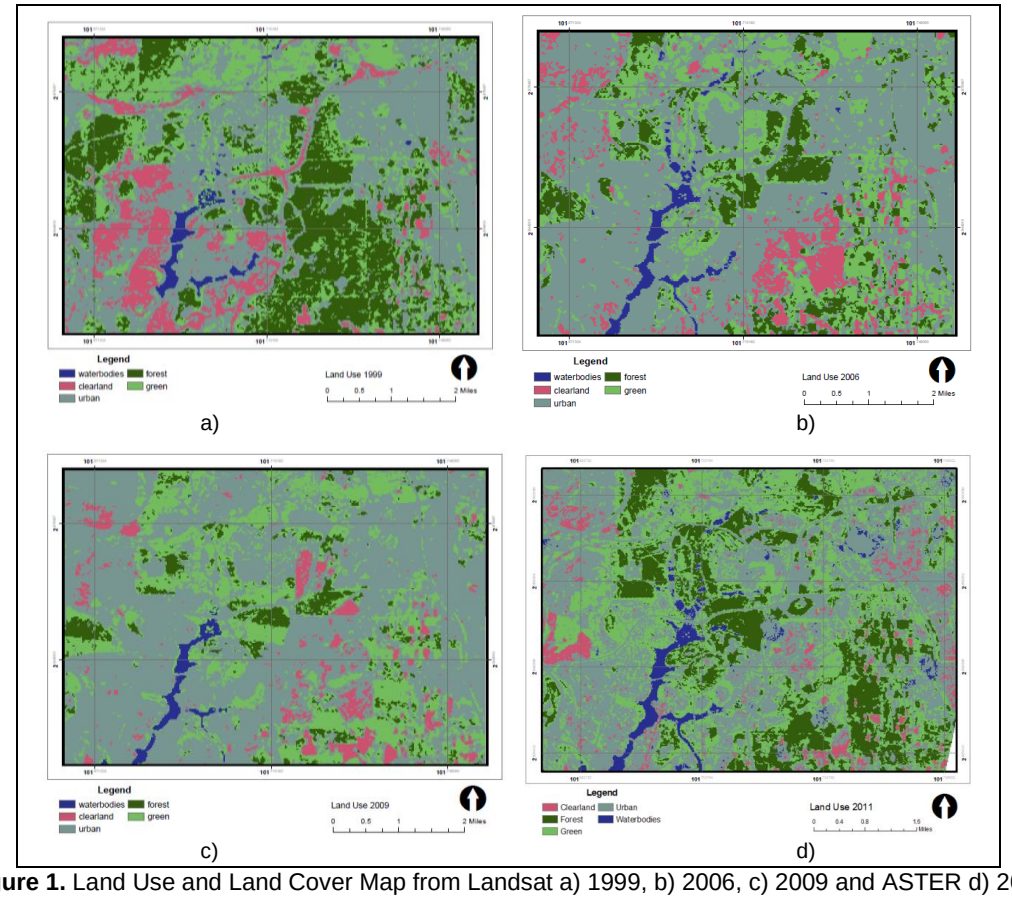

Figure 1. Land Use and Land Cover Map from Landsat a) 1999, b) 2006, c) 2009 and ASTER d) 2011 (Adapted from Salleh et al. (2013))

The land use map of year 2011 shows some significant increments and improvements towards greenery and forest land. However, the forested land here can be categorised as dense vegetation, which is resulted from the transformation of young landscapes and green surfaces in the study area. Most of the clear land area in 2009 has been converted into both green or dense areas and also urban areas. As the source image used in generating the land use 2011 map has a different spatial resolution, the comparison was performed by looking at the percentage area of land use of the image coverage. Figure 2 shows the changes of land use percentages for Putrajaya for 1999, 2006, 2009 and 2011. This Figure consists of two doughnut charts representing the temporal changes of land use at the specified dates, and also at more consistent intervals (1999, 2009 and 2011). The consistent intervals reduce the variations of land use change patterns.

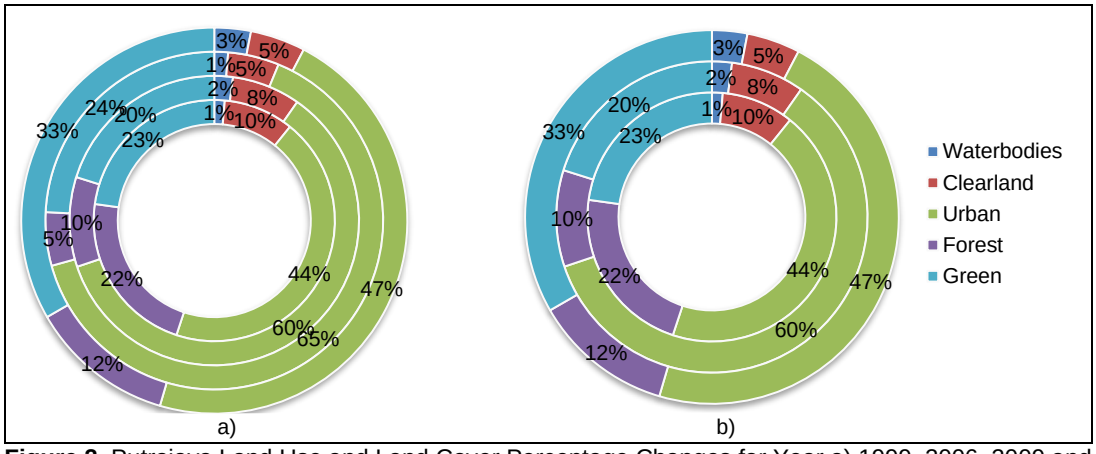

Figure 2. Putrajaya Land Use and Land Cover Percentage Changes for Year a) 1999, 2006, 2009 and 2011; and b) 1999, 2006 and 2011

There are extensive lists of albedo research conducted all over the world mentioned in Salleh et al. (2012); however, only recently a few of these research stressed tropical regions (Salleh et al., 2012a; 2012b), particularly in Malaysia. Land covers influence the percentage reflectance of radiation (Li et al., 2012) and several scientists have performed regional studies and suggested that different geographical settings affect the magnitude of reflectance toward climate change effects (Krishna et al., 2022; Qinqin et al., 2021; Sung and Li, 2012). The albedo was suggested to be increased during dry seasons consistent with the transformation of canopies to the leafless canopies and the influences of dry and bright soil (Sieber et al., 2022). As can be seen and concluded from previous studies, the gap within land surface albedo study is the non-existence of this study in the tropical and sub-tropical region and how it was being neglected in many of climate change research. Hence, this study will provide a generous insight on how land surface albedo behaves within tropical and sub-tropical regions and whether there is any significant difference between land surface albedo values across different types of land use land cover. Particularly, in looking the at the impacts of land surface albedo and temperature dynamics towards local scale weather and meteorological condition in which can further be use for climate change study. Based on this study, perhaps a novel approach of quantification and modelling of land surface albedo at a local scale for weather and climate research can be established.

METHODOLOGY

Emerging geospatial technology application for urban studies can be seen in Isa et al. (2018). Thus, the methodology adopted in this study is illustrated as in Figure 3.

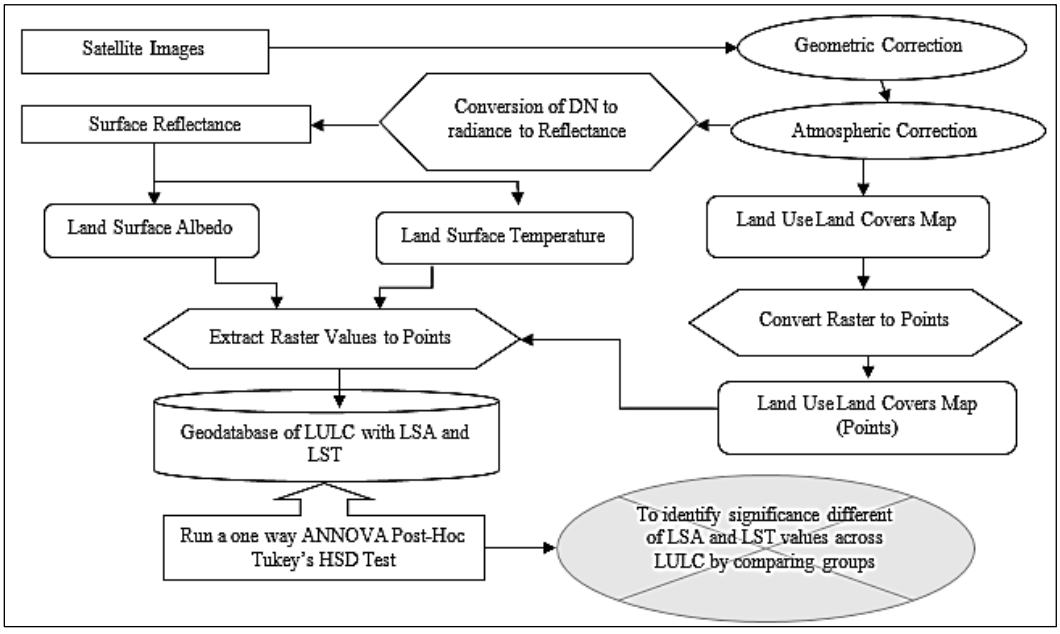

Figure 3. The Methodological Flow Diagram

Three main data used in this investigation were LSA, LST and LULC of satellite images captured on 12 December 1999, 2 December 2006, 21 January 2009 and 19 January 2011. Each of these images undergoes atmospheric and geometric corrections and further processed to become LSA, LST and LULC maps. The data used in this study is mainly raster dataset that is converted into GIS point layer. The LULC point layer is used to extract the raster values representing the LSA and LST of each of the gridded pixel of the study area. The final merged geo-database layer consists of the ranging from 70000 to 111000 thousand of pixels of categorical LULC classes with extracted centre pixel of LSA and LST values in each of the tuple.

Remote Sensing Techniques for Land Surface Albedo and Land Surface Temperature

The depiction of remotely sensed LSA is based on the method by Liang (2004) for Landsat LSA and Mokhtari et al. (2013) for ASTER very near infrared (VNIR) band.

$$Landsat\ LSA = 0.356\alpha\_1 + 0.130\alpha\_2 + 0.373\alpha\_4 + 0.085\alpha\_5 + 0.072\alpha\_7 - 0.0018 \quad (1)$$

$$ASTER_{VNIR}\ LSA = 0.697\alpha_1 + 0.298\alpha_3 + 0.008 \quad (2)$$

Notes:

LSA = Land Surface Albedo
ASTER = The Advanced Spaceborne Thermal Emission and Reflection Radiometer
VNIR = Visible Near InfaRed
α = Albedo

Prior to extracting the LST, images have undergone atmospheric correction to remove the effects of the atmosphere. The Dark Object Subtraction algorithm is applied by using the COST method (Chavez, 1996). Then the parameters are translated into Spatial Models in the ERDAS Imagine software (Leica Geosytem). Two methods for LST extraction were applied in this study known as Split Window (Mao et al., 2005) and Mono Window (Qin et al., 2001). The typical steps are similar in both methods except for the final equation arrangements (see Equation 7). The sequential processes performed to compute LST from ASTER and Landsat TM starts with converting the spectral radiance to at-sensor brightness temperature, computing the transmittance equation, and then correcting the spectral emissivity. Finally, calculations of the LST are conducted using the Split and Mono Window methods. The equations utilised in this study are Atmospheric Correction COST Method (Chavez, 1996) - All TM bands (except band 6) need to be atmospherically corrected to reduce the atmospheric effects in the image. Using the COST Method (Chavez, 1996), the image undergoes atmospheric correction according to this equation:

$$\rho Band_N = \frac{\pi[(LBand_N * GainBand_N + BiasBand_N) - (HBand_N * BiasBand_N)] * D^2}{EBand_N * [cos((90 - \theta) * \pi/180)]} \quad (3)$$

Where,

$\rho Band_N$ = Reflectance for Band N
$LBand_N$ = Digital Number for Band N
$HBand_N$ = Dignal Number representing Dark Object for Band N
$EBand_N$ = Solar Irradiance for Band N
D = Normalised Earth-Sun Distance

Conversion from Digital Number (DN) to Radiance - All TM bands are stored in DN with their ranges from 0 to 255. The data are then converted to radiance using a linear equation (Sobrino et al., 2004):

$$CV_R = G\ (CV_{DN}) + B \quad (4)$$

Where:

CV_R = The cell value as radiance
CV_{DN} = The cell value digital number
G = The gain (0.005632156 for TM6)
B = The offset (0.1238 for TM6)

This equation can be simply written as follow:

$$L = L_{min} + (L_{max} - L_{min})\ {}^{Q_{dn}}/_{Q_{max}} \quad (5)$$

Where,

Lmin = minimum at-sensor spectral radiance
Lmax = maximum at-sensor spectral radiance
Qdn = DN value of pixel
Qmax = maximum DN value of pixels

Conversion from radiance to brightness temperature - By applying the inverse of the Planck function with two free parameters (Schott and Volchok, 1985; Wukelic et *al.*, 1989), the spectral radiances are converted into satellite brightness temperature using the following relationship.

$$T = \frac{K_2}{\ln\left(\frac{K_1}{CV_R} + 1\right)} \tag{6}$$

Where,

T = Temperature in Kelvin
CV_R = the cell value as radiance
K_1 = TM Calibration constant 1 (607.76)
K_2 = TM Calibration constant 2 (1260.56)

Land surface temperature retrieval - Land surface temperature is derived based on the brightness temperature data. The conversion is carried out using the following equation (Qin et al., 2001),

$$Ts = \frac{[a(1 - C - D) + [b(1 - C - D) + C + D]\, T_i - DT_a]}{C} \tag{7}$$

Where,

Ts = Land surface temperature
a = −67.355351
b = 0.458606
C = $\mathcal{E}i \times \tau atm$
D = $(1 - \tau atm)\,[1 + (1 - \mathcal{E}i) \times \tau atm]$
Ti = at-sensor temperature
Ta = mean atmospheric temperature

Several other values are required in order to be able to generate LST from the Mono-Window equation. For certain parameters, the atmospherically corrected bands are needed (TM4 and TM5). Therefore, the Normalised Difference Vegetation Index, Emissivity, Estimation Atmospheric transmittance and mean atmospheric temperature need to be calculated as they are required as input in the LST retrieval equation.

The simplest form of vegetation index is a ratio between near infrared and red reflectance, named Simple Ratio (SR). For healthy living vegetation, this ratio will be high due to the inverse relationship between vegetation brightness in the red and infrared regions of the spectrum. Based on the geometrically corrected Landsat ETM+ images the SR can be calculated by using this formula.

$$SR = \frac{\rho red}{\rho nir} \tag{8}$$

Where the ρ*nir* is the reflectance of the near infrared band (Band 4 of Landsat ETM+) and the ρ*red* is the reflectance of the red band (Band 3 of Landsat ETM+). The Normalised Difference Vegetation Index (NDVI) is the most widely used vegetation index. It can be calculated by using this equation.

$$NDVI = \frac{(\rho nir + \rho red)}{(\rho nir - \rho red)} \tag{9}$$

Emissivity is calculated using an equation established by Sobrino et al. (2004),

$$\varepsilon_i = 0.004P_V + 0.986 \tag{10}$$

Where, *Pv* is the vegetation proportion (Carlson and Ripley, 1997) obtained from this equation:

$$Pv = \frac{NDVI - NDVI_{min}}{NDVI_{max} - NDVI_{min}} \tag{11}$$

Estimation of atmospheric transmittance is determined using Equation 12, where *w6* can be referred from the distribution of water vapour content graph (Qin et al., 2001).

$$\tau atm = 1.031412 - 0.11536 \times w6 \tag{12}$$

The mean atmospheric temperature is then computed using Equation 13, where to is the mean air temperature

$$\mathrm{Ta} = 17.9769 + 0.91715 \times \mathrm{To} \tag{13}$$

Statistical Analysis

The generated land surface albedo and LULC maps are used to test if there are significant differences of albedo values with respect to land use classes. For this test, the Post-Hoc Tukey's HSD was selected to assist one way ANOVA to determine the respective groups. The one-way ANOVA compares the means between the groups one is interested in and determines whether any of those means are significantly different from each other. Specifically, it tests the null hypothesis. The formula for Tukey's HSD is written as follows:

$$HSD = q\sqrt{MSE/n*} \tag{14}$$

Where q = the relevant critical value of the studentised range statistic and n^* is the number of scores used in calculating the group means of interest. If, however, the one-way ANOVA returns a significant result, the alternative hypothesis (H_A) will be accepted, which is that there are at least two group means that are significantly different from each other.

VALIDATION OF REMOTELY SENSED LAND SURFACE ALBEDO (LSA)

The retrieved LSA values (Figure 4) are validated using a method established by Salleh et al. (2014) with reference to the available CAQMs and meteorological AWs within the study area. To increase the number of points for validation, the whole coverage scene is used instead of the portion of the scene that represents the study area (Figure 5). The yellow points show the locations of the CAQMs and meteorological AWs location within the study area.

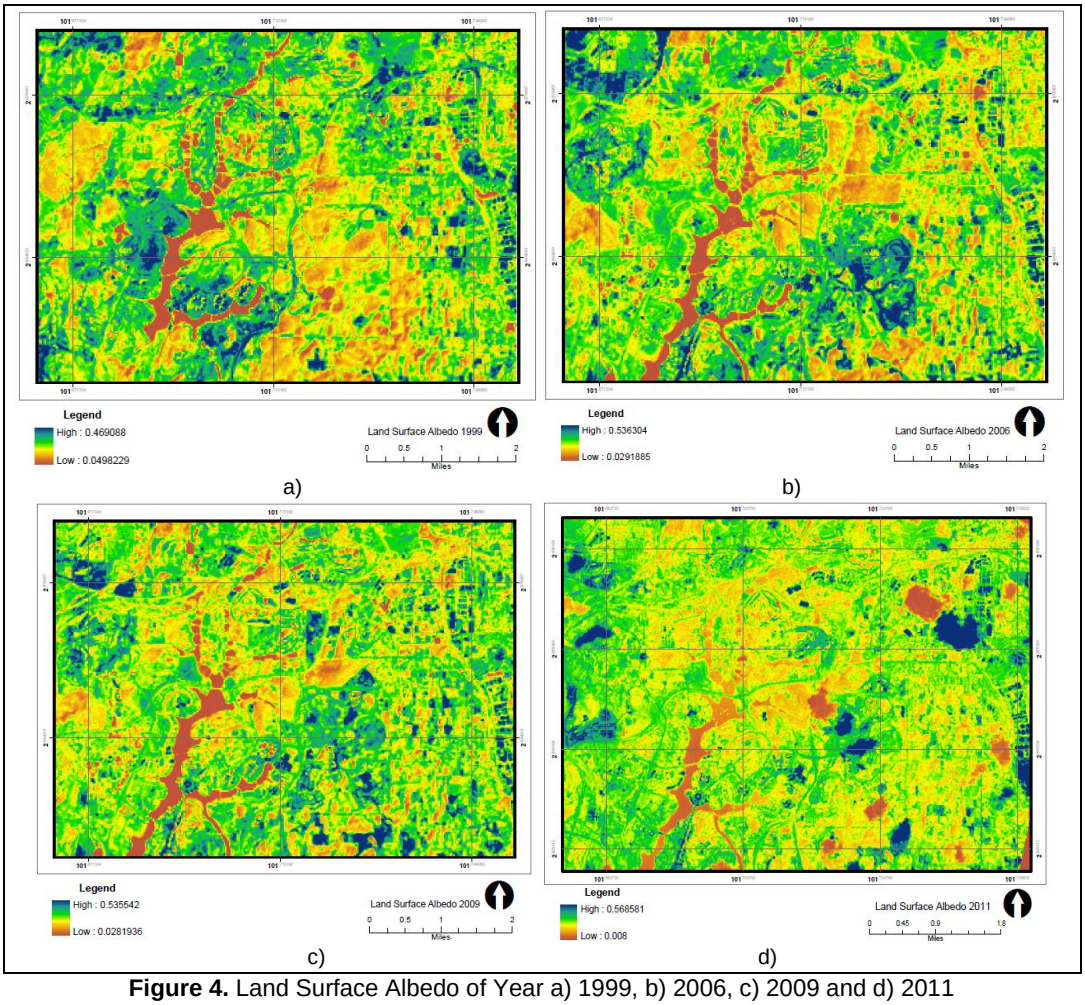

Figure 4. Land Surface Albedo of Year a) 1999, b) 2006, c) 2009 and d) 2011

Tables 1 show the values of remotely sensed LSA as compared to the relative true values. The relative validation for 2011 LSA is performed using ten (10) observation locations comprising of five (5) CAQM stations, two (2) meteorological AW stations and three (3) in-situ observations. While for 2009 LSA, there were seven (7) stations used for validation but only five (5) ambient temperature values are available for LSA estimation. In 2006, there were only six (6) daily ambient temperatures available out of seven (7) stations and finally for the year 1999, as the CAQMs had only been established in 2000, the relative validation of LSA is performed utilising ambient temperature values from meteorological AW stations. Using inputs from Tables 1 to 4, the relative standard error (RSE), root mean square error (RMSE), mean square error (MSE) and mean absolute error (MAE) are calculated.

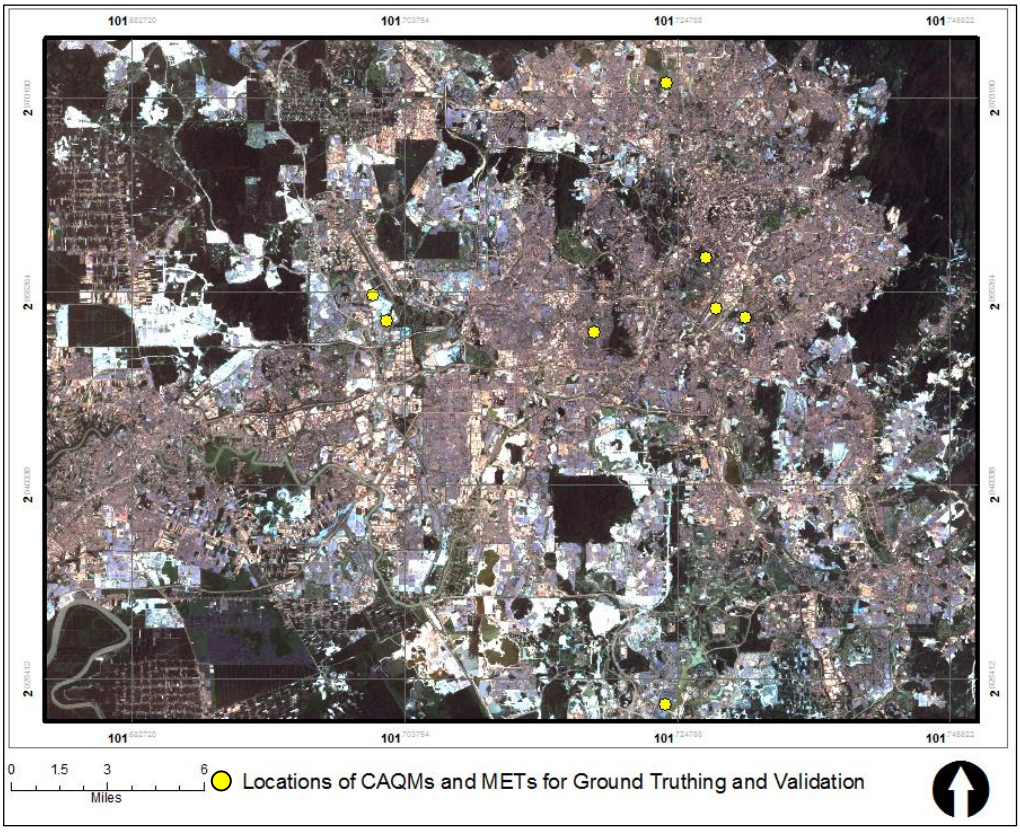

Figure 5. The Location of CAQMs and AWs used for Ground-Based Validation

Table 2 shows the RSE, RMSE, MSE and MAE of the relative true values of LSA and the specified years used for the time series analyses. It can be concluded that there are some variations in the magnitude of error since the RMSE values are larger than MAE. The same magnitude errors are indicated if the RMSE value is equal to MAE. However, since the value differences between RMSE and MAE are not big, large errors are unlikely to have occurred. Based on the MAE values, the average differences between observed and predicted values of LSA are within a range of 0.01 to 0.07.

Table 1. The Ground-Based LSA to Remotely Sensed LSA (1999-2011)

LOCATION	1999				2006				2009				2011			
	N*ii*	Landsat	°C	*d*	N*ii*	Landsat	°C	*d*	N*ii*	Landsat	°C	*D*	N*ii*	Vnir	°C	*d*
Putrajaya CAQMs	*Null*	0.198	*null*	*null*	0.210	0.227	24.8	-0.017	0.201	0.187	25.86	0.014	0.145	0.259	32.83	-0.114
Bt. Muda CAQMs	*Null*	0.174	*null*	*null*	*Null*	0.177	*Null*	*Null*	*Null*	0.178	*Null*	*Null*	0.144	0.229	33	-0.085
P. Jaya CAQMs	*Null*	0.179	*null*	*null*	0.203	0.185	25.6	0.023	0.206	0.175	25.26	0.031	0.137	0.235	33.83	-0.098
Shah Alam CAQMs	*Null*	0.212	*null*	*null*	0.202	0.201	25.8	0.001	0.188	0.157	27.56	0.030	0.172	0.240	24.79	-0.030
Cheras CAQMs	*Null*	0.218	*null*	*null*	0.206	0.197	25.2	0.010	*Null*	0.169	*Null*	*Null*	0.190	0.246	27.2	-0.089
P. Jaya AWs	0.184	0.205	28	-0.02049	0.175	0.181	29.1	-0.006	0.192	0.163	27	0.029	0.177	0.192	28.9	-0.015
Subang AWs	0.184	0.248	28	-0.06425	0.175	0.206	29.1	-0.030	0.193	0.173	26.9	0.020	0.185	0.237	27.9	-0.052

**d* representing differences

Table 2. The Accuracy Assessment and Reliability Test for Remotely Sensed LSA

YEAR	RSE (%)	RMSE ($\sqrt{MSE}$)	MSE	MAE
1999	4.2365	0.0476815	0.002273528	0.042365
2006	1.4391667	0.0175579	0.00030828	0.01439167
2009	2.47986	0.025697	0.000660336	0.0247986
2011	6.51335	0.0715771	0.005123281	0.0651335

Statistically, the values of RMSE, RSE, MSE and MAE are within the tolerance outlined by Browne et al. (1993). However, Henderson-Sellers and Wilson (1983) and Sellers et al. (1995) have documented the absolute requirements for datasets suitable for evaluating climate model demand for land surface albedo, with the level of uncertainty ranging from 0.02 to 0.05. As such, by evaluating both RMSE and MAE values; the 2006 image is selected to be used as the case study to test the relationship of remotely sensed LSA with other selected variables due to it having the lowest scores of MAE and RMSE, indicating a better fit with LSA values depicted from the remote sensing image. With reference to the recent study on examining and evaluating the MODIS and Landsat albedo with in-situ observations (Román et al., 2013; Wang et al., 2014), the findings in this section show good agreement to using Landsat to quantify LSA in subtropical regions such as Malaysia.

The land surface temperature (LST) is another biophysical parameter chosen in this study. The LST for this study is generated using Landsat thermal bands (1999, 2006 and 2009) and ASTER (2011). The LST are generated through the Mono-window method. Figure 5.8 shows the temporal changes of remotely sensed LST from 1999 to 2011. The urbanised and built-up area, with a light-yellow tone towards orange and red colour in Figure 6, indicated a warmer surface temperature. These areas spread dramatically from 1999 to 2006, suggesting the expansion of UHI. However, a slight decrease can be seen in 2009, which calls for further investigation to comprehend this situation.

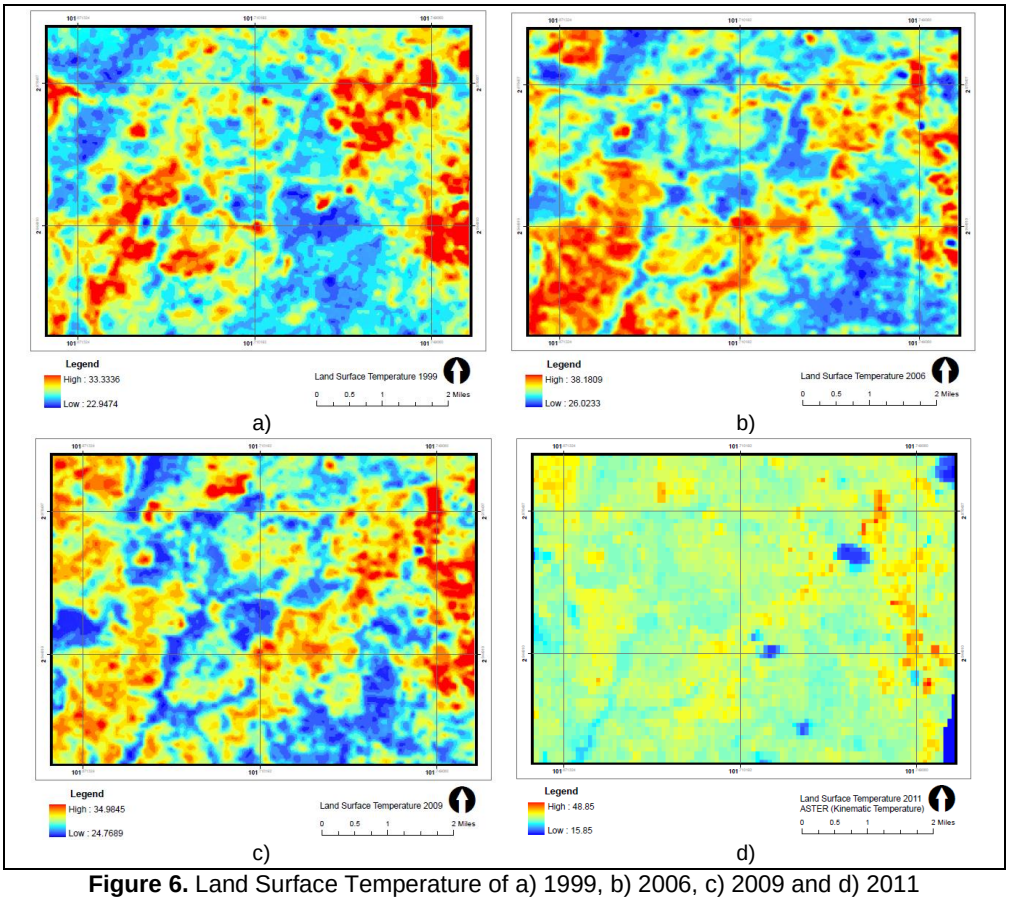

Figure 6. Land Surface Temperature of a) 1999, b) 2006, c) 2009 and d) 2011

RESULTS AND DISCUSSION

The value of LSA can be very surface specific. Using LULC maps generated through remote sensing images, the raster images are converted into point layers. Based on each of these layers, each centre pixel value of land use class and LSA are extracted and tabulated. By using SPSS for Windows software, the following tables show the descriptive land use statistics of the study area for the years 1999, 2006, 2009 and 2011.

The MSE for all years are relatively small throughout the land use and land cover categories (0.0001 – 0.0007). In the year 1999, the highest standard deviation of LSA belongs to the urban built up class (0.0348), while 2006 showed clear land scored the biggest standard deviation at 0.0328. In the LSA values for 2009, the largest deviation occurs to LSA values belonging to clear land (0.0371) and is repeated in 2011 where the standard deviation of LSA for clear land is 0.0644. Tables 3 and 4 represent the mean LSA for all land use land cover classes of the study area. Further to this, Tables 5 and 6 show the derived land surface temperature according to the 5 (five) land use land cover classes.

From Tables 5 and 6, the mean LST of land use over the study does not deviate very much from each other. From the year 1999 to 2011, the standard deviations of LST are between 0.8 and 3.5, which reveal the highest deviation came from LST depicted from an ASTER image in 2011. The LST standard errors across the land use and land covers classes are also very low comparatively, with the lowest standard error at 0.007 seen in 1999, 2006 and 2009 which all fall into the urban built up land use land cover class. The highest LST standard error is for water bodies in 2011 with 0.04775. Although the standard error and standard deviation are comparatively low throughout the land use and land cover classes, they do have significant differences in terms of the maximum and minimum temperature of LST. In 1999, the maximum urban surface temperature seems to be lower than for vegetative land. This indicates the albedo and evapotranspiration effects. The same pattern is depicted in 2009. It is found to contradict from common knowledge of having the built-up surface warmer than vegetative land. This behaviour is clearly seen in 2006.

Table 7 demonstrates the mean of LSA and LST according to the land use and land cover classes of the study area. Evidently, both the LSA and LST are generally lower over forested land than over greenery grassland. Clear land has considerably higher albedo than urban areas. Water bodies obviously possesses the lowest surface albedo values. Land surface albedo retrieved from remotely sensed data requires an understanding towards the land use land cover conversion and ecosystem disturbance affected the surface energy balance (Shuai et al., 2011). Therefore, pattern recognition of LSA and LST in accordance with land use and land cover is importance.

Table 3. LSA According to Land Use (1999 and 2006)

Land use Type		1999							2006						
		N	Min	Max	Mean		Std. D	Var	N	Min	Max	Mean		Std. D	Var.
		Statistic			Stat	Std. E	Statistic		Statistic			Stat	Std. E	Statistic	
Clear Land	Land Surface Albedo	8336	.1208	.3691	.2175	.0004	.0315	.001	6693	.1203	.3280	.2166	.0004	.0328	.001
	Valid N (listwise)	8336							6693						
Forest	Land Surface Albedo	19594	.0769	.2326	.1610	.0001	.0160	.000	8885	.0945	.2117	.1330	.0001	.0114	.000
	Valid N (listwise)	19594							8885						
Greenery Grassland	Land Surface Albedo	20185	.0673	.2875	.1884	.0002	.0228	.001	17793	.1090	.2466	.1676	.0002	.0199	.000
	Valid N (listwise)	20185							17793						
Urban Built-Up	Land Surface Albedo	39226	.0498	.4691	.1883	.0002	.0348	.001	51740	.0435	.3476	.1699	.0001	.0291	.001
	Valid N (listwise)	39226							51740						
Water Bodies	Land Surface Albedo	1232	.0573	.1622	.0757	.0003	.0111	.000	1086	.0414	.1823	.0728	.0005	.0161	.000
	Valid N (listwise)	1232							1086						

Table 4. LSA According to Land Use (2009 and 2011)

Land use Type		2009							2011						
		N	Min	Max	Mean		Std. D	Var	N	Min	Max	Mean		Std. D	Var.
		Statistic			Stat	Std. E	Statistic		Statistic			Stat	Std. E	Statistic	
Clear Land	Land Surface Albedo	4367	.1160	.4360	.2160	.0006	.0371	.001	8681	.1843	.5263	.3032	.0007	.0644	.004
	Valid N (listwise)	4367							8681						
Forest	Land Surface Albedo	4539	.0891	.2065	.1315	.0002	.0142	.000	32536	.1316	.2880	.1963	.0001	.0135	.000
	Valid N (listwise)	4539							32536						
Greenery Grassland	Land Surface Albedo	21456	.0332	.2321	.1406	.0002	.0269	.001	67828	.1540	.3403	.2191	.0001	.0165	.000
	Valid N (listwise)	21456							67828						
Urban Built-Up	Land Surface Albedo	57228	.0327	.5355	.1576	.0001	.0275	.001	93267	.1185	.5655	.2289	.0002	.0517	.003
	Valid N (listwise)	57228							93267						
Water Bodies	Land Surface Albedo	1168	.0282	.1086	.0393	.0002	.0075	.000	4764	.1295	.2243	.1576	.0002	.0123	.000
	Valid N (listwise)	1168							4764						

Table 5. Derived Land Surface Temperature for Each Land Use Type 1999 and 2006

Land use Type		1999							2006						
		N	Min	Max	Mean		Std. D	Var	N	Min	Max	Mean		Std. D	Var.
			Statistic		Stat	Std. E	Statistic			Statistic		Stat	Std. E	Statistic	
Clear Land	LST	8302	23.0202	31.7546	26.0439	.0146	1.3323	.775	6766	27.6587	35.5987	30.8499	.0162	1.3281	1.764
	Valid N (listwise)	8302							6766						
Forest	LST	19471	23.3947	31.7478	26.2441	.0098	1.3599	1.849	8885	26.9972	34.4483	29.1872	.0085	.8044	.647
	Valid N (listwise)	19471							8885						
Greenery Grassland	LST	20072	23.3970	33.3336	26.2159	.0101	1.4350	2.059	17832	27.5065	35.5309	30.0050	.0088	1.1680	1.364
	Valid N (listwise)	20072							17832						
Urban Built-Up	LST	39080	22.9474	32.2834	26.1592	.0070	1.3920	1.938	53256	26.0233	38.1809	31.9620	.0072	1.6717	2.795
	Valid N (listwise)	39080							53256						
Water Bodies	LST	1234	22.9666	29.0674	25.2789	.0333	1.1705	1.370	1837	27.5994	33.0019	29.4405	.0187	.8032	.645
	Valid N (listwise)	1234							1837						

Table 6. Derived Land Surface Temperature for Each Land Use Type 2009 and 2011

Land use Type		2009							2011						
		N	Min	Max	Mean		Std. D	Var	N	Min	Max	Mean		Std. D	Var.
			Statistic		Stat	Std. E	Statistic			Statistic		Stat	Std. E	Statistic	
Clear Land	LST	4294	24.7783	33.9391	28.6876	.0262	1.7192	.956	8672	16.8500	45.8500	33.3644	.0366	3.4065	11.604
	Valid N (listwise)	4294							8672						
Forest	LST	4502	25.3324	34.9845	28.8336	.02647	1.7758	.153	32527	16.8500	47.8500	32.8179	.0141	2.5407	6.455
	Valid N (listwise)	4502							32527						
Greenery Grassland	LST	21212	25.1724	34.9463	28.7169	.0106	1.5445	.386	67771	15.8500	47.8500	32.8992	.0116	3.0179	9.108
	Valid N (listwise)	21212							67771						
Urban Built-Up	LST	56994	24.7689	34.9666	28.9337	.0070	1.6739	.802	93069	15.8500	47.8500	33.1324	.0117	3.5628	12.693
	Valid N (listwise)	56994							93069						
Water Bodies	LST	1157	25.1673	32.3484	28.0430	.0410	1.3948	.946	4748	16.8500	47.8500	32.0975	.0477446	3.2899	10.823
	Valid N (listwise)	1157							4748						

Table 7. Mean LSA and LST (°C)

Land Cover	Land Surface Albedo			
	1999	**2006**	**2009**	**2011**
Water bodies	0.07582	0.06762	0.039278	0.15764
Clearland	0.21750	0.21777	0.216108	0.30321
Urban	0.18831	0.16929	0.157541	.228922
Forest	0.16102	0.13295	0.131428	0.19630
Greenery Grass Land	0.18839	0.16769	0.140647	0.21912
Land Cover	**Land Surface Temperature (°C)**			
	1999	**2006**	**2009**	**2011**
Water bodies	25.27888	29.44054	28.04295	32.09747
Clearland	26.04394	30.84987	28.68758	33.36441
Urban	26.15916	31.96199	28.93368	33.13239
Forest	26.24409	29.18722	28.83363	32.81793
Greenery Grass Land	26.21590	30.00504	28.71689	32.89924

Land surface temperatures across different land cover in 1999 appear to be the lowest, ranging from 25°C to 27°C. The variations of land cover land surface temperature in 2006 are noticeably larger as compared to the years 1999, 2009 and 2011. Forested land appears to have the lowest temperature (29.19°C) while the surface temperature of urban areas is the highest (31.96°C). Smaller variances of land surface temperature between 28°C – 29°C and 32°C - 33°C are depicted in 2009 and 2011 respectively. Such variations are probably due to the seasonal local heterogeneity of specific dates when the images are being captured (Shuai et al., 2011), surface soil texture and geological characteristics like albedo and emissivity are evidently related in terms of their spatial pattern and magnitude (Zhou et al., 2003) and also the process of extracting LSA from satellite images, such as the overly corrected atmospheric effects. The fluctuations of LSA with respect to LST are illustrated in Figure 7.

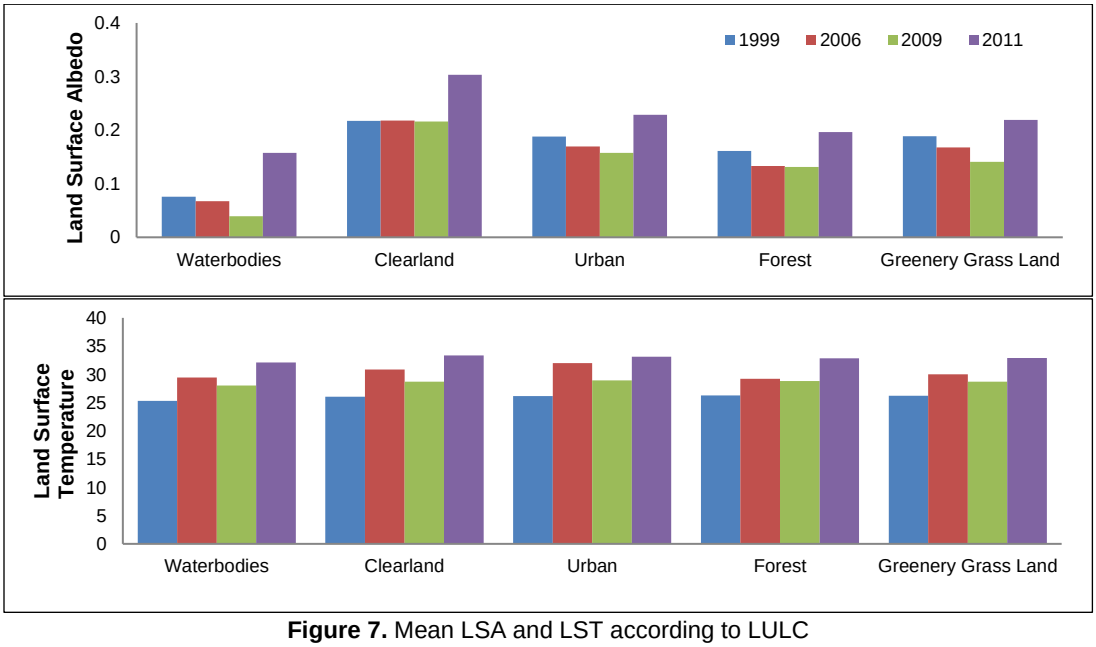

Figure 7. Mean LSA and LST according to LULC

A single factor ANOVA with post-hoc Tukey's HSD test is executed to see if any significant differences of LSA are present across the land covers. In order to test for significant difference between the albedo and temperature values associated with the land covers within and between each image, the Tukey's honesty significant difference (HSD) test is executed using a 0.00048 significance level in order to minimise the experiment wise error rate. There are 25 pairings for each land cover within an image performed. The significant difference of LST and LSA across LULC will be able to calibrate many weather and climate simulation studies. Especially at local scale where LULC may have been largely generalised. LSA is also capable in supressing the air and land surface temperature, thus, this finding may change perception towards the use of high albedo (reflective) material for built up area. The physical behaviour of high reflective materials can also help reducing the impacts of climate change especially with respect to surface heat and global warming (Hamoodi et al., 2019).

All of the land covers in image 1999 have significantly different ($p < 0.00048$) land surface albedo and surface temperature values, except when comparing Group 3 (Urban) and Group 5 (Greenery Grass Land) albedo values where $p = 0.998$ (± 0.0000758), $p < 0.00048$, and Group 4 (forest) and Group 5 (Greenery Grass Land) land surface temperature values with $p = 0.256$ (± 0.0281855), $p < 0.00048$. Table 8 demonstrates the Single way ANOVA for year 1999. All of the land covers in image 2006 have statistically significant different ($p < 0.00048$) land surface albedo and surface temperature values. While in 2009, all land covers have significantly different ($p < 0.00048$) land surface albedo, except when comparing the land surface temperature values of Group 2 (Clear Land) and Group 5 (Greenery Grass Land) where $p = 0.826$ (± 0.0293095), $p < 0.00048$, and Group 3 (Urban) and Group 4 (forest) where $p = 0.001$ (± 0.1000526), $p < 0.00048$. Tables 8 and 9 show the single-way ANOVA for years 2006 and 2009 respectively.

All of the land covers in image 2011 have significantly different ($p < 0.00048$) land surface albedo and surface temperature values, except when comparing the land surface temperature of Group 4 (Forest) and Group 5 (Greenery Grass Land) where $p = 0.002$ (± 0.0813049), $p < 0.00048$. Table 9 presents the single-way ANOVA for year 2011.

Table 11. Single ANOVA Tukey' s HSD Year 1999 and 2006

		1999					2006				
		SS	df	MS	F	Sig.	SS	df	MS	F	Sig.
LSA	Between Groups	35.125	4	8.781	10880.274	.000	46.170	4	11.542	12756.681	.000
	Within Groups	71.148	88154	.001			80.140	88571	.001		
	Total	106.274	88158				126.310	88575			
LST	Between Groups	1265.106	4	316.276	164.512	.000	98695.968	4	24673.992	11381.346	.000
	Within Groups	169476.688	88154	1.923			192015.959	88571	2.168		
	Total	170741.794	88158				290711.928	88575			

Table 12. Single ANOVA Tukey' s HSD Year 2009 and 2011

		2009					2011				
		SS	df	MS	F	Sig.	SS	df	MS	F	Sig.
LSA	Between Groups	38.554	4	9.639	13048.092	.000	103.367	4	25.842	17264.202	.000
	Within Groups	65.119	88154	.001			309.519	206782	.001		
	Total	103.673	88158				412.886	206786			
LST	Between Groups	1642.324	4	410.581	151.179	.000	8405.003	4	2101.251	201.107	.000
	Within Groups	239414.248	88154	2.716			2160543.893	206782	10.448		
	Total	241056.572	88158				2168948.896	206786			

With respect to the above discussions, the image for 2006 is found to have LSA and LST values across the land use land covers scoring statistical significance and the image for 2011 has good statistical significance consistency of its LSA across the land use and land covers. Figure 8 shows the relationships between LSA and LST mean values with regards to the LULC in 2006.

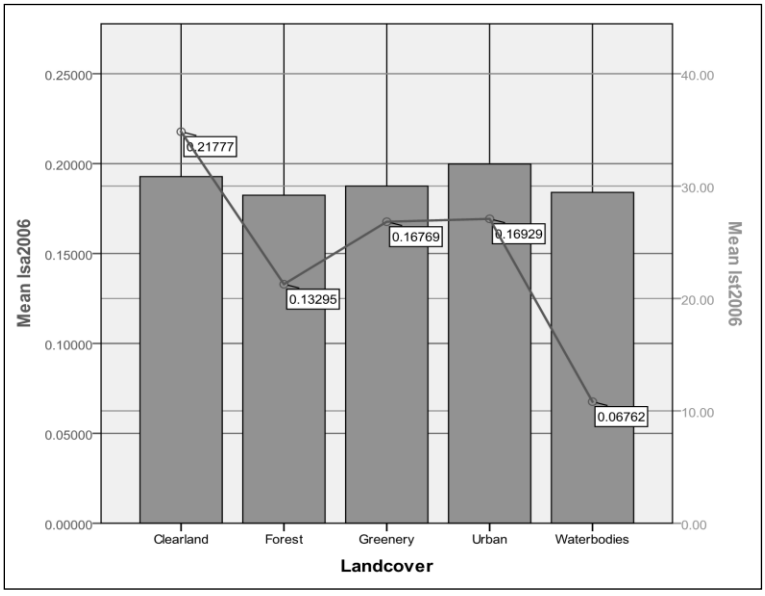

Figure 8. Mean LSA and LST of Different LULC 2006

The highest LSA is captured in clear land areas, followed by the urban area. Water bodies has the lowest mean LSA (0.06762 ± .0003975), with LSA increasing over mixed greenery grassland. Even with two of the highest mean shortwave (SW) albedos, the clear land and built-up land covers also has two of the highest average surface temperatures (30.84987 ± .0161457 °C and 31.96199 ± .0072439 °C). Here, the exterior factors that influenced the values of LST and LSA can be inferred as the LST and LSA relate contradictory (increased in LST decreased in LSA). Figure 8 illustrated that the land use may moderating the fluctuation of LSA and LST values.

CONCLUSION

The study focused in determining the significant difference of LSA and LST based on different land use land cover. A single factor ANOVA with Tukey's HSD test is executed to see if any significant differences of LSA and LST are present between the land covers. It is identified that there are significant differences in term of values of LSA and LST across the LULC. In the year 1999, the LSA of Groups 3 and 5 are not statistically significant (mean difference of ±0.0000756) and the LST of Groups 4 and 5 differences were also not statistically significant (mean difference of ±0.0281855). For the year 2009, the LST of Groups 2 and 5, and 3 and 4 are not statistically significant with mean differences of ±0.0293095 and ±0.1000526 respectively. As for 2006, the LSA and LST of all groups of land cover appeared to be statistically significant while in 2011 only one LST comparison (Groups 4 and 5) appeared to be statistically not significant with a mean difference of

±0.0813049. These findings exhibits that the land surface albedo quantification is important not only to the snow-covered region but also snow-free region, specifically referred to this study at the subtropical region such as Malaysia. Therefore, it is crucial to capture the actual values of LSA especially when this biophysical variable is been classified as an Essential Climate Variable (ECV). However, it is also recommended to justify the important of this finding by conducting relevant climate simulation that involve with LSA in order to be able to quantify the impacts and magnitude of which these statistically significant difference to the climate modelling and simulation results. A new approach of extracting land surface albedo data via google earth engine can also be explored to furnish the climate researcher with more accessible information about land surface albedo (Capolupo et al., 2021).

ACKNOWLEDGEMENTS

The author would like to gratefully acknowledge financial support from Universiti Teknologi MARA and the Ministry of Higher Education under the Fundamental Research Grant Scheme (FRGS), FRGS/1/2019/WAB03/UITM/02/1 and Universiti Teknologi MARA (UiTM) with collaboration from Univeristy of Nottingham, Malaysia Campus for enabling this research to be carried out. The Landsat TM data are available from the U.S. Geological Survey (USGS).

REFERENCES

Browne, M. W., Cudeck, R., Bollen, K. A., and Long, J. S. (1993). Alternative ways of assessing model fit. *Sage Focus Editions, 154*, 136-136.

Buyantuyev, A., and Wu, J. (2010). Urban heat islands and landscape heterogeneity: linking spatiotemporal variations in surface temperatures to land-cover and socioeconomic patterns. *Landscape Ecology, 25*(1), 17-33.

Capolupo, A., Monterisi, C., Sonnessa, A., Caporusso, G., & Tarantino, E. (2021, September). Modeling land cover impact on albedo changes in Google Earth Engine environment. In International Conference on Computational Science and Its Applications (pp. 89-101). Springer, Cham

Carlson, T. N., and Ripley, D. A. (1997). On the relation between NDVI, fractional vegetation cover, and leaf area index. *Remote Sensing of Environment, 62*(3), 241-252.

Chavez, P. S. (1996). Image-based atmospheric corrections-revisited and improved. *Photogrammetric Engineering and Remote Sensing, 62*(9), 1025-1035.

Feng, H., Xiong, J., Ye, S., Zou, B., & Wang, W. (2022). Vegetation Change Enhanced the Positive Global Surface Radiation Budget. Advances in Space Research.

Hamoodi, M. N., Corner, R., & Dewan, A. (2019). Thermophysical behaviour of LULC surfaces and their effect on the urban thermal environment. *Journal of Spatial Science*, 64(1), 111-130.

Henderson-Sellers, A., and Wilson, M. (1983). Surface albedo data for climatic modeling. *Reviews of Geophysics, 21*(8), 1743-1778.

Isa, N. A., Salleh, S. A., Wan Mohd, W. M. N., & Chan, A. (2018). Kuala Lumpur City of Tomorrow: Integration of Geospatial Urban Climatic Information In City Planning. *Theoretical and Empirical Researches in Urban Management, 13*(4), 5-27.

Krishna, S. S., Prijith, S. S., Kumar, R., Sai, M. S., & Ramana, M. V. (2022). Planetary albedo decline over Northwest India contributing to near surface warming. *Science of The Total Environment*, 816, 151607.

Li, H., Harvey, J., and Kendall, A. (2012). Field measurement of albedo for different land cover materials and effects on thermal performance. *Building and Environment*.

Mao, K., Tang, H., Chen, Z., Qiu, Y., Qin, Z., and Li, M. (2005). A split-window algorithm for retrieving land-surface temperature from ASTER data. *Remote Sensing Information*, 7-11.

Qin, Z., Karnieli, A., and Berliner, P. (2001). A mono-window algorithm for retrieving land surface temperature from Landsat TM data and its application to the Israel-Egypt border region. *International Journal of Remote Sensing*, *22*(18), 3719-3746.

Qinqin, L., Yichen, T., Kai, Y., Feifei, Z., Chao, Y., & Guang, Y. (2021). Spatio-Temporal Pattern of Surface Albedo in Beijing and Its Driving Factors Based on Geographical Detectors. *Journal of Resources and Ecology*, 12(5), 609-616.

Román, M. O., Gatebe, C. K., Shuai, Y., Wang, Z., Gao, F., Masek, J. G., He, T., Liang, S., and Schaaf, C. B. (2013). Use of In Situ and Airborne Multiangle Data to Assess MODIS- and Landsat-Based Estimates of Directional Reflectance and Albedo. *IEEE Transactions on Geoscience and Remote Sensing, IEEE Transactions on*, *51*(3), 1393-1404.

Salleh, S. A., Abd Latif, Z., Wan Mohd, W. M. N., and Chan, A. (2012a). *Air quality parameters dependency of remotely-sensed albedo.* Paper presented at the IEEE 8th International Colloquium on Signal Processing and its Applications (CSPA), 2012.

Salleh, S. A., Abd Latif, Z., Wan Mohd, W. M. N., and Chan, A. (2012b). Albedo Pattern Recognition and Time-series Analyses in Malaysia. *Int. Arch. Photogramm. Remote Sens. Spatial Inf. Sci.*, *XXXIX-B7*(2012), 6. doi: 10.5194/isprsarchives-XXXIX-B7-235-2012

Salleh, S. A., Latif, Z. A., Pradhan, B., Wan Mohd, W. M. N., & Chan, A. (2014). Functional relation of land surface albedo with climatological variables: a review on remote sensing techniques and recent research developments. *Geocarto International*, 29(2), 147-163.

Sellers, P., Meeson, B., Hall, F., Asrar, G., Murphy, R., Schiffer, R., Bretherton, F., Dickinson, R., Ellingson, R., and Field, C. (1995). Remote sensing of the land surface for studies of global change: Models—algorithms—experiments. *Remote Sensing of Environment*, *51*(1), 3-26.

Shuai, Y., Masek, J. G., Gao, F., and Schaaf, C. B. (2011). An algorithm for the retrieval of 30-m snow-free albedo from Landsat surface reflectance and MODIS BRDF. *Remote Sensing of Environment*, *115*(9), 2204-2216.

Sieber, P., Ericsson, N., Hammar, T., & Hansson, P. A. (2022). Albedo impacts of current agricultural land use: Crop-specific albedo from MODIS data and inclusion in LCA of crop production. *Science of The Total Environment*, 155455.

Sobrino, J. A., Jimenez-Munoz, J. C., and Paolini, L. (2004). Land surface temperature retrieval from LANDSAT TM 5. *Remote Sensing of Environment*, *90*(4), 434-440.

Sung, C. Y., and Li, M. H. (2012). Considering plant phenology for improving the accuracy of urban impervious surface mapping in a subtropical climate regions. *International Journal of Remote Sensing*, *33*(1), 261-275.

Wang, Z., Schaaf, C. B., Strahler, A. H., Chopping, M. J., Román, M. O., Shuai, Y., Woodcock, C. E., Hollinger, D. Y., and Fitzjarrald, D. R. (2014). Evaluation of MODIS albedo product (MCD43A) over grassland, agriculture and forest surface types during dormant and snow-covered periods. *Remote Sensing of Environment*, *140*, 60-77.

Zhou, L., Dickinson, R., Ogawa, K., Tian, Y., Jin, M., Schmugge, T., and Tsvetsinskaya, E. (2003). Relations between albedos and emissivities from MODIS and ASTER data over North African Desert. *Geophys. Res. Lett*, *30*(20), 2026.